Molecular structure and vibrational spectra of methyl cyanoacetate: an FT-IR, Raman and ab initio molecular orbital study

2 AUTHORS, INCLUDING:

Rui Fausto
University of Coimbra

330 PUBLICATIONS **4,525** CITATIONS

Molecular structure and vibrational spectra of methyl cyanoacetate: an FT-IR, raman and ab initio molecular orbital study

João Miguel F. Neta, Rui Fausto*

Departamento de Química, Universidade de Coimbra, P-3049 Coimbra, Portugal

Received 6 August 1997; revised 15 September 1997; accepted 15 September 1997

Abstract

The results of a combined vibrational and structural study of methyl cyanoacetate undertaken by Raman and infrared spectroscopy, and ab initio SCF-MO calculations are presented. It is shown that for the isolated molecule situation, as well as in the liquid phase, methyl cyanoacetate exists as a mixture of two main conformers of similar energies, differing by the relative orientation of the NC–C–C=O axis (the *syn* and *skew* forms, having a NC–C–C=O dihedral angle equal to 0° and in the ± 140° region, respectively). In the crystalline state, only the thermodynamically most stable *syn* conformer remains. The ab initio SCF-MO optimized geometries of the various possible conformers, their relative stabilities, dipole moments and harmonic force-fields are presented, and the conformational dependence of some relevant structural parameters is used to characterise the most important intramolecular interactions present in the various forms studied. Finally, results of a normal mode analysis based on the ab initio calculated vibrational spectra are used to help interpret the experimental vibrational data, enabling a detailed assignment of both Raman and infrared spectra. © 1998 Elsevier Science B.V.

Keywords: Methyl cyanoacetate; Molecular structure; Infrared spectrum; Raman spectrum; Molecular orbital calculations

1. Introduction

Methyl cyanoacetate [N≡(CCH$_2$C(=O)OCH$_3$; MCA] is currently used both as an intermediate in pharmaceutically oriented synthetic chemistry and as a starting material for the industrial production of some herbicides and bactericides [1]. However, despite its relevant industrial importance, this compound has not been deserved much attention in the past. The first study dealing with the conformational isomerim in MCA was published almost 20 years ago [2]. In that study, a first attempt was made to interpret the infrared spectra of liquid and crystalline MCA, as

well as those obtained for this molecule in CCl$_4$ or CS$_2$ diluted solutions, in terms of the presence of two relevant conformational states (the *syn* form, where the NC–C–C=O dihedral angle is equal to 0°, and the *skew* conformer, where this angle should be close to ± 120°; in both cases the ester group was assumed to adopt the *s-cis* conformation, Fig. 1). The *syn* conformer was assumed to be the most stable form in all phases studied, and the energy difference between the two conformers estimated to be 4.06 kJ mol^{-1}, in the pure liquid (in the crystal only the bands ascribed to the most stable form could be observed) [2]. More recently, however, the conformational equilibrium of MCA was reinvestigated by a combined infrared spectroscopy and P.C.I.L.O. theoretical
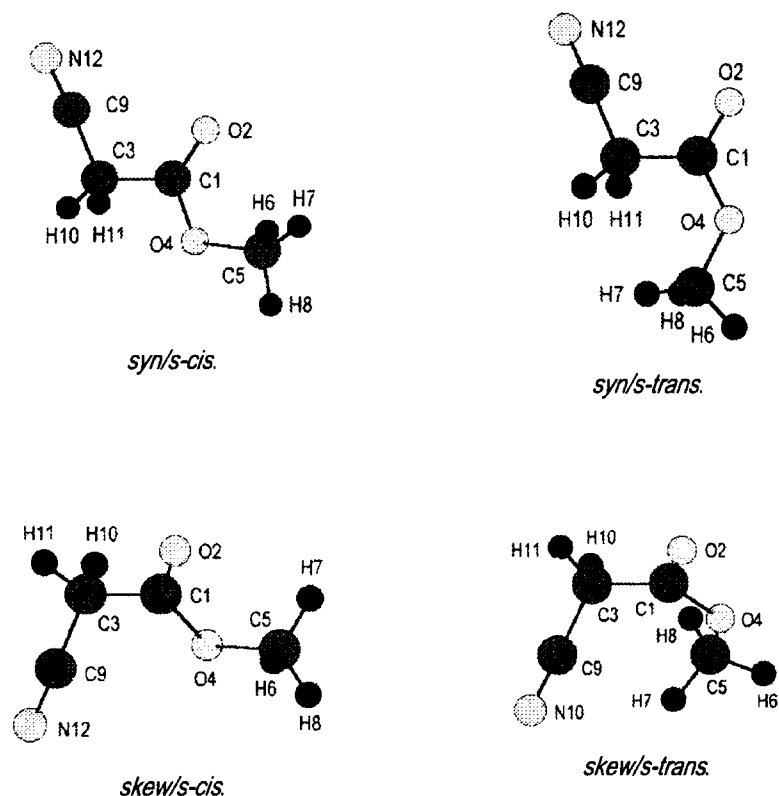
* Corresponding author.

Fig. 1. Conformers of methyl cyanoacetate and atom numbering scheme. The two *s-cis* forms correspond to the two single conformers considered in all previous studies of MCA [2–4].

approach [3], and the relative energy of the two observed conformers was estimated to be considerably lower than that previously reported ($\Delta E_{skew-syn}$ = 1.46 kJ mol^{-1} [3]). In addition, the P.C.I.L.O. calculations predicted the *skew* form as the ground conformational state for the isolated molecule situation ($\Delta E_{skew-syn}$ = − 2.13 kJ mol^{-1} [3,4]).

In all previous studies [2–4], however, neither the evaluation of precise molecular geometries of the different possible conformers of MCA nor a detailed analysis of the vibrational spectra of this molecule were undertaken. Moreover, it appeared to be essential, in order to enable the establishment of fundamental structure/spectra correlations and to evaluate the most relevant intramolecular interactions present in the various conformers of methyl cyanoacetate, that this molecule should be the subject of a systematic structural and vibrational study by means of a higher level theoretical approach. Thus, in order to fill this gap, in this article we report the results of a combined

vibrational spectroscopy (Raman and infrared) and ab initio SCF-MO study carried out on MCA.

2. Experimental and computational methods

Spectroscopic grade methyl cyanoacetate (99.9%) was obtained from Aldrich and purified by conventional methods prior to spectra recording.

Infrared spectra were obtained using a Nicolet FTIR 800 system equipped for the 4000–400 cm^{-1} region with a germanium on CsI beam splitter and a deuterated triglycine sulphide (DTGS) detector with CsI windows. Data collection was performed using a specially designed demountable transmission variable temperature liquid cell with KBr windows, linked to a VENTACON (Winchester) model CAL 9000 temperature controller. For each spectrum 32 scans were recorded with the spectral resolution 1 cm^{-1} and coadded.

Raman spectra were obtained using a modified Harney–Miller variable temperature sampling system in a SPEX 1403 double monochromator spectrometer (focal distance 0.85 m, aperture/7.8), equipped with holographic gratings with 1800 grooves mm^{-1} (ref. 1800-1SHD). The 514.5 nm argon laser (Spectra-Physics, model 164-05) line, adjusted to provide 220 mW power at the sample, was used as excitation radiation. Detection was effected using a thermoelectrically cooled Hamamatsu R928 photomultiplier. Spectra were recorded using increments of 1 cm^{-1} and integration times of 1 s. Under these conditions, the estimated errors in wavenumbers are 1 cm^{-1}.

The ab initio molecular orbital calculations were performed using the 6-31G* basis set [5] with the GAUSSIAN92/DFT program package [6] running on a DEC ALPHA 7000 computer. Molecular geometries were fully optimised by the force gradient method using Berny's algorithm [7]. The largest residual coordinate forces were always less than 3×10^{-4} hartree bohr^{-1} (1 hartree = 2625.5001 kJ mol^{-1}; 1 bohr = 5.29177×10^{-11} m) or hartree rad^{-1}, for bond stretches and angle bends, respectively. The stopping criterion for the SCF iterative process required a density matrix convergence of less than 10^{-8}. The force constants (symmetry internal coordinates) to be used in the normal coordinate analysis were obtained from the ab initio cartesian harmonic force constants using the program TRANSFORMER (version 2.0) [8]. This program was also used to prepare the input data for the normal coordinate analysis programs used in this study (BUILD-G and VIBRAT [9]).

3. Results and discussion

3.1. Geometries and relative energies

Methyl cyanoacetate has two internal axes of rotation that can lead to conformational isomers. These correspond to rotations about the C1–O4 and C1–C3 bonds. On the other hand, the preferred orientation of the ester group in methyl esters is well known to be that where one of the hydrogen atoms stands in the anti periplanar position relative to the carbonyl carbon atom [10–12] (Fig. 1).

Conformational isomerism about the C–O single bond in carboxylic acids and esters has been studied in detail previously [10–14]. It is now well established that these compounds adopt preferentially the s-cis conformation about this bond (O=C–O–R dihedral angle equals to 0; R = H or alkyl), except when strong steric hindrance dominates. The energy difference between this conformation and the second stable form (the s-trans conformer, corresponding to a O=C–O–R dihedral angle equal to 180°) and the energy barrier for interconversion between these two forms are usually very large (over 20 and 40 kJ mol^{-1}, respectively [10–16]). The main factors which determine the much lower energy of the s-cis O=C–O–R axis when compared with that of the s-trans O=C–O–R axis are the presence in the first of the strongly stabilising through-space field interaction resulting from the nearly antiparallel alignment of the C=O and O–R bond dipoles, and the destabilising steric interactions between the R group and the acyl fragment in the s-trans form [13]. In general, s-trans conformers are not observed spectroscopically under current experimental conditions, unless particular specific intramolecular stabilising interactions are operating (e.g. intramolecular hydrogen bonding in chloroacetic acid monomer [16,17]). However, s-trans-like conformations have been recently proposed as catalytically important conformational states [18], thus justifying the interest in studying s-trans conformational states of carboxylic compounds as well.

The conformational isomerism in α-substituted carbonyl compounds related with the internal rotation about the bond made by the α and the carbonyl carbon atoms (C$_\alpha$–C) is associated, in general, with relatively low energy barriers and conformer energy differences, and has been extensively studied in our laboratory for a series of different α-carbon substituents [12,13,15,16]. In the case of alkyl esters adopting the s-cis conformation about the C–O bond, the internal rotation about the C$_\alpha$–C bond in mono-substituted compounds originates two different, by symmetry, conformers (the syn and skew forms, Fig. 1) whose relative energy difference is in general quite small [12,13,15,19,20]. Most of the time, the C$_s$ symmetry syn conformer is slightly more stable than the doubly degenerated by symmetry C$_1$ skew form, in particular when the α-substituents are relatively volumous or electronegative [10,12,20]. For s-trans (C–O)-like ester molecules, the appearance of stable conformations having a non-planar skeleton is common, which

essentially result from the strong steric interactions between the alkyl ester moiety and the acyl group [10,12,20]. The main factors responsible for the relative stabilities of the conformations interconvertible by internal rotation about the C_α–C bond in carboxylic compounds have been discussed in detail elsewhere [10,12,19,20], being essentially due to (i) the larger effective volume and more negative charge of the – O– atom when compared with the carbonyl oxygen, (ii) several specific electronic effects that, besides

depending upon the properties of the carboxylic group, also depend on the nature of the substituent (mesomerism [13,15], hyperconjugation [19,20], inter-fragment HOMO/LUMO interactions [10,19]), and (iii) intramolecular hydrogen bonding [12,16,19].

The theoretical calculations undertaken in this study were able to identify four distinct conformers of MCA (Fig. 1). The calculated geometries and relative energies of these conformers are presented in Table 1. As expected, the conformers having an

Table 1
6-31G* calculated optimised geometries and energies for the various conformers of methyl cyanoacetate

| Parameter[a] | Conformer | | | |
	syn/s-cis	syn/s-trans	skew/s-cis	skew/s-trans
	bond length/pm			
C1O2	118.23	117.79	118.50	118.04
C1C3	151.71	152.64	151.97	153.17
C1O4	131.93	132.70	131.31	132.19
O4C5	142.16	141.02	142.21	141.52
C5H6	107.99	107.80	107.97	107.78
C5H7	107.99	108.28	107.99	108.00
C5H8	107.79	108.28	107.75	108.27
C3C9	146.68	146.63	146.89	147.02
C3H10	108.36	108.39	108.51	108.36
C3H11	108.36	108.39	108.03	107.97
C9N12	113.36	113.30	113.39	113.43
	bond angle/degrees			
C3C1O2	125.53	122.85	122.53	120.23
O2C1O4	125.03	120.62	125.14	120.75
C3C1O4	109.43	116.52	112.32	119.01
C1O4C5	116.90	124.05	117.23	124.31
O4C5H6	110.28	105.58	110.19	105.30
O4C5H7	110.28	111.60	110.21	111.45
O4C5H8	105.67	111.60	105.60	111.32
C1C3C9	113.19	112.34	114.16	113.30
C1C3H10	108.79	110.13	107.92	111.14
C1C3H11	108.79	110.13	108.16	106.40
C3C9N12	182.46	182.91	181.41	180.22
	dihedral angle/degrees			
O4C3C1O2	180.00	180.00	177.15	179.00
C5O4C1C3	180.00	0.00	178.98	3.92
H6C5O4C1	60.53	180.00	59.61	175.23
H7C5O4C1	60.53	61.76	61.48	66.25
H8C5O4C1	180.00	61.76	179.02	57.35
C9C3C1O2	0.00	0.00	141.02	114.03
H10C3C1O2	121.95	121.11	98.38	123.37
H11C3C1O2	121.95	121.11	18.41	5.48
	conformer energy/kJ mol^{-1}			
ΔE[b]	0.00	45.99	0.94	44.40

[a] See Fig. 1 for atom numbering.

[b] Energies relative to the most stable conformer; values presented include zero-point vibrational energy corrections. The total energy for the most stable form is, – 358.5616241 (E_h).

s-cis (C–O) axis are considerably more stable than the s-trans forms. In addition, for a given conformation of the C–O axis, the two conformers differing in the orientation of the cyano group relative to the carbonyl group (syn and skew forms) have similar energies. Contrary to the results previously obtained by using the P.C.I.L.O. method [3,4], the higher level ab initio calculations predict the syn/s-cis form as corresponding to the conformational ground state for the isolated molecule situation (the zero-point-energy corrected $\Delta E_{(skew/s-cis)-(syn/s-cis)}$ energy difference was found to be 0.94 kJ mol^{-1}; Table 1). Essentially, the slightly higher energy of the skew/s-cis form when compared with the syn/s-cis conformer results from the more important repulsive interactions between the cyano group (that has a relatively large electron density due to its triple bond) and the lone-electron pairs of the ester oxygen, that is both more negatively charged and more volumous than the carbonyl oxygen [11,12,20]. These stronger cyano/–O– repulsions in the skew/s-cis form when compared with the cyano/O= repulsions are clearly reflected in the longer C≡N, C_α–C and O–C(H$_3$) bond lengths, and in the larger C–C–C, C–C–O and C–O–C angles found in the skew/s-cis form (Table 1). On the other hand, in the case of the two high energy s-trans (C–O) conformers, the syn form about the C_α–C axis is less stable than the skew form by ca. 1.6 kJ mol^{-1}. This relative destabilisation of the syn conformation about the C_α–C axis associated with the change in conformation about the C–O bond can be easily explained considering the extra repulsive interactions due to the close proximity of the two methylene hydrogen atoms from the two out-of-plane methyl hydrogens in the syn/s-trans conformer, that have no counterpart either in the syn/s-cis or in the skew/s-trans forms (Fig. 1). In addition, the possible existence of a weak intramolecular hydrogen bond involving one of the methyl hydrogens and the C≡N triple bond in the skew/s-trans form may also contribute to the observed inversion of the syn (C_α–C) versus skew (C_α–C) axis stability upon changing from the s-cis to the s-trans (C–O) configuration, though the above mentioned repulsive interaction is certainly the most important factor. A similar hydrogen bond interaction, but that time involving the considerably stronger OH/C≡N intramolecular hydrogen bond, was found to operate in the monomer of cyanoacetic acid, being the most important factor in

stabilizing the anti/s-trans conformer of this molecule relative to the syn/s-trans form [1].

In general, the changes in geometric parameters with the s-cis → s-trans isomerisation follow the typical pattern of variation for these kind of systems [10–16] and do not require here any additional comments: e.g. the C=O bond length reduces while the C–O bond length increases, due to the reduced importance in the s-trans forms of the mesomerism associated with the ester group, the O=C–O and C–O–C angles reduce, since in the s-cis forms the molecular heavy atom backbone must open to make way for the methyl group. In turn, besides the structural changes already referred to above that originate in the different strengths of the cyano/–O– and cyano/O= repulsions, the syn → skew isomerization about the C_α–C bond does not lead to any additional relevant change in the geometric parameters, though the C=O bond length is slightly longer in skew than in syn conformers (Table 1). This slight increase in the C=O bond length may be explained, at least in part, considering that the closest proximity of the positively charged methylene hydrogens from the carbonyl oxygen atom, in the skew forms, gives rise to an electron charge flux from the C=O bonding region towards this atom, thus leading to a weakening of the C=O bond in these conformers.

3.2. Charge distribution analysis

Table 2 shows the ab initio calculated Mulliken atomic charges and dipole moments for the various conformers of MCA.

Following the general parttern for this kind of molecule [11,13–16], s-trans conformers have a considerably higher dipole moment than the corresponding s-cis forms. This result is a direct consequence of the relative orientation of the C=O and O–C(H$_3$) bond dipoles in s-cis and s-trans conformers and, as referred to previously, have important energetic implications, favouring the s-cis forms (where the rough-space field interaction associated with the two bond dipoles is attractive). In addition, as previously predicted from vector addition of bond moments and MNDO semiempirical calculations [3], for a given configuration of the ester group, the syn conformer has a higher dipole moment than the skew form. The experimental dipole moment of MCA

Table 2
6-31G* Mulliken atomic charges and dipole moments for the various conformers of methyl cyanoacetate[a]

| | Conformer | | | |
	syn/s-cis	syn/s-trans	skew/s-cis	skew/s-trans
	charge/e			
C1	0.7995	0.8154	0.7981	0.8050
O2	−0.5319	−0.4947	−0.5502	−0.5095
C3	−0.4641	−0.5134	−0.4513	−0.4955
O4	−0.6115	−0.5966	−0.5896	−0.5857
C5	−0.1932	−0.2006	−0.1944	−0.2122
H6	0.1927	0.2222	0.1934	0.2172
H7	0.1927	0.1732	0.1896	0.2044
H8	0.1943	0.1732	0.1993	0.1684
C9	0.3390	0.3501	0.3202	0.3143
H10	0.2629	0.2552	0.2614	0.2506
H11	0.2629	0.2552	0.2682	0.2846
N12	−0.4434	−0.4393	−0.4447	−0.4418
	dipole moment/Debye			
$|\mu|$	5.71	7.16	2.95	4.25

[a] $e = 1.6021892 \times 10^{-19}$ C; 1 Debye $= 3.336 \times 10^{-3}$ C.m.

(in benzene solution) is 3.74 D [3] (1 D = 3.33564 × 10^{-3} C.m), a value that may be compared with the ab initio calculated values for the two most stable conformers (syn/s-cis: 5.7 1 D; skew/s-cis: 2.95 D).

From the calculated Mulliken atomic charges for the various conformers, the following correlations can be drawn:

1. For all conformers, the charge of the ester oxygen atom is predicted to be more negative than that of the carbonyl oxygen. This result follows the usual pattern previously observed for this kind of molecule and, as explained elsewhere [14], is essentially due to the larger π electron population of the –O– atom when compared with that of the carbonyl oxygen, while the σ electron population of these two oxygen atoms follows the inverse order.

2. For a given conformation of the NC–C–C=O axis, the charge on the carbonyl oxygen atom is systematically more negative in the s-cis conformer than in the s-trans form. Such a result correlates with the prevalence in the first forms of the through-space field interaction between the C=O and O–C(H₃) bond dipoles already mentioned. Moreover, this effect also explains the relative charges on C5 for s-trans and s-cis conformers, that are systematically less negative in the later.

3. For a given configuration of the ester group, the charge of the carbonyl oxygen atom is more negative in the skew than in the syn form. This can be considered as a consequence of the electron charge flux from the C=O bonding region towards the carbonyl oxygen, that occurs upon syn → skew isomerisation, due to the presence, in the later form, of the positively charged methylene hydrogen atoms in the close vicinity of the carbonyl oxygen. Such a result reinforces the explanation given above to interpret the slight increase observed in the C=O bond length upon syn → skew isomerisation.

4. Finally, the charges of the hydrogen atoms (in particular, H10, H11, H7 and H8) attain their less positive values in the syn/s-trans conformer, reflecting the strong electrostatic repulsion between these atoms in this form.

3.3. Vibrational spectra

MCA has 30 fundamental vibrations. In the case of the C_s symmetry conformers (syn forms), the normal modes will span the irreducible representations, 19A′ + 11A″, while those of the non-symmetric skew forms (C_1 point group) belong to the A symmetry species. Hence, all vibrations are active in both Raman and infrared. Table 3 presents the definition of the internal symmetry coordinates used in this study. The

Table 3
Definition of the internal symmetry coordinates used in normal coordinate analysis

Coordinate	Symmetry[a]	Approximate description	Definition[b]
S_1	A'	$\nu C=O$	$\nu C=O$
S_2	A'	$\nu C1-C3$	$\nu C1-C3$
S_3	A'	$\nu C1-O$	$\nu C1-O$
S_4	A'	$\nu C3-C9$	$\nu C3-C9$
S_5	A'	$\nu C\equiv N$	$\nu C\equiv N$
S_6	A''	$\nu CH_2 as$	$(\nu C-H10) - (\nu C-H11)$
S_7	A'	$\nu CH_2 s$	$(\nu C-H10) + (\nu C-H11)$
S_8	A'	$\nu O-C5$	$\nu O-C5$
S_9	A'	$\nu CH_3 as'$	$2(\nu C-H8) - (\nu C-H7) - (\nu C-H6)$
S_{10}	A''	$\nu CH_3 as''$	$(\nu C-H7) - (\nu C-H6)$
S_{11}	A'	$\nu CH_3 s$	$(\nu C-H8) + (\nu C-H7) + (\nu C-H6)$
S_{12}	A'	$\delta O=C-O$	$2(\delta O=C-O) - (\delta CC=O) - (\delta CC-O)$
S_{13}	A'	$\delta CC=O$	$(\delta CC=O) - (\delta CC-O)$
S_{14}	A'	$\delta C-O-C$	$\delta C-O-C$
S_{15}	A'	$\delta CH_3 as'$	$2(\delta H6-C-H7) - (\delta H6-C-H8) - (\delta H7-C-H8)$
S_{16}	A''	$\delta CH_3 as''$	$(\delta H6-C-H8) - (\delta H7-C-H8)$
S_{17}	A'	$\delta CH_3 s$	$(\delta H6-C-H8) + (\delta H7-C-H8) + (\delta H6-C-H7) - (\delta O-C-H8) -$ $(\delta O-C-H7) - (\delta O-C-H6)$
S_{18}	A'	$\gamma CH_3'$	$2(\delta O-C-H8) - (\delta O-C-H7) - (\delta O-C-H6)$
S_{19}	A''	$\gamma CH_3''$	$(\delta O-C-H7) - (\delta O-C-H6)$
S_{20}	A'	γCH_2	$5(\delta H10-C-H11) - (\delta CCC) - (\delta C1-C3-H10) - (\delta C1-C3-H11) -$ $(\delta C9-C3-H10) - (\delta C9-C3-H11)$
S_{21}	A'	ωCH_2	$(\delta C1-C3-H10) + (\delta C1-C3-H11) - (\delta C9-C3-H10) - (\delta C9-C3-H11)$
S_{22}	A''	tw CH_2	$(\delta C1-C3-H10) - (\delta C1-C3-H11) - (\delta(C9-C3-H10) +$ $(\delta C9-C3-H11)$
S_{23}	A''	γCH_2	$(\delta C1-C3-H10) - (\delta C1-C3-H11) + (\delta C9-C3-H10) - (\delta C9-C3-H11)$
S_{24}	A'	δCCC	$4(\delta CCC) - (\delta C1-C3-H10) - (\delta C1-C3-H11) - (\delta C9-C3-H10) -$ $(\delta C9-C3-H11)$
S_{25}	A'	$\delta CC\equiv N$	$\delta CC\equiv N$
S_{26}	A''	$\gamma C=O$	$\gamma C=O$
S_{27}	A''	$\gamma CC\equiv N$	$\delta CC\equiv N$
S_{28}	A''	$\tau C1-O$	$\tau C1-O$
S_{29}	A''	$\tau C1-C3$	$\tau C1-C3$
S_{30}	A''	$\tau O-CH_3$	$\tau O-CH_3$

[a] Symmetry refers strictly to C_s conformers. For the non-symmetric C_1 forms, all coordinates belong to the A symmetry species.

[b] Normalisation constants are not given here; they are chosen as $N = (\Sigma C_i^2)^{-1/2}$, where C_i are the coefficients of the individual valence coordinates. Vibrations: ν, bond stretching; δ, bending; ω, wagging; tw, twisting; γ, rocking; τ, torsion; as., asymmetric; s., symmetric.

observed and theoretically predicted spectra are shown in Figs. 2–6, and the vibrational assignments summarised in Table 4. Table 5 presents the results of the theoretical vibrational calculations for the non-observed s-trans conformers. All the calculated frequencies shown correspond to scaled values, obtained by multiplying the ab initio values by a single scale factor (0.9). While very simple, this scaling procedure preserves the potential energy distributions (PEDs) as they emerge from the ab initio calculations, thus having an important advantage over the more elaborate force field scaling procedures that use more than one

scale factor, that usually give rise to important PED distortions from the ab initio calculated values.

3.4. Region above 1700 cm^{-1}

This is the spectral region where the $\nu C-H$ (five modes: νCH_2 as., νCH_2 s., νCH_3 s. and the two νCH_3 as. vibrations), $\nu C\equiv N$ and $\nu C=O$ stretching modes occur.

The assignments of both $\nu C\equiv N$ and $\nu C=O$ are straightforward, since these modes give rise to bands in well defined and practically clear spectral regions.
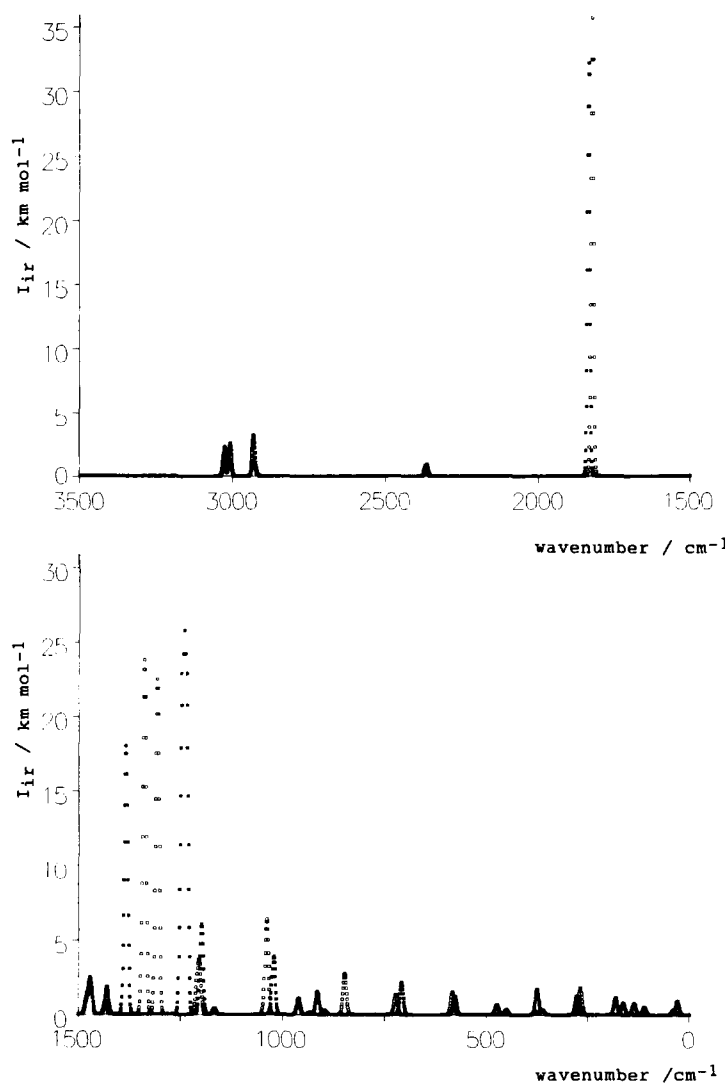
Fig. 2. 6-31G* calculated IR spectra of the two spectroscopically observed conformers of MCA: ■ *syn/scis*; □ *skew/s-cis*. The calculated intensities of the bands due to the *syn/s-cis* conformer are multiplied by the factor 1.12 to account for the relative population of the two conformers at room temperature (see text). All gaussian functions used to simulate the bands are arbitrarily chosen to have a half band width equal to 10 cm^{-1}.

The calculations predict that these vibrations should appear at slightly higher frequencies in the *syn/s-cis* conformer, but, for the liquid sample, it was not possible to resolve the νC=O band into the two components originated in individual conformers. However, in consonance with this result, the νC=O band blueshifts upon crystallisation (1762 cm^{-1}), clearly reflecting the fact that, in this later situation, only the more polar *syn* conformer exists. On the other hand, νC≡N appears as an overlapping doublet of bands, whose temperature dependence enables us to assign the higher frequency conponent to the *skew* form. Despite the fact that the order of appearance of the bands is not the same as predicted by the calculations, this assignment is reinforced by the crystalline state data, since despite several bands which appear in the corresponding spectral region due to overtone or/and combination modes, the main band
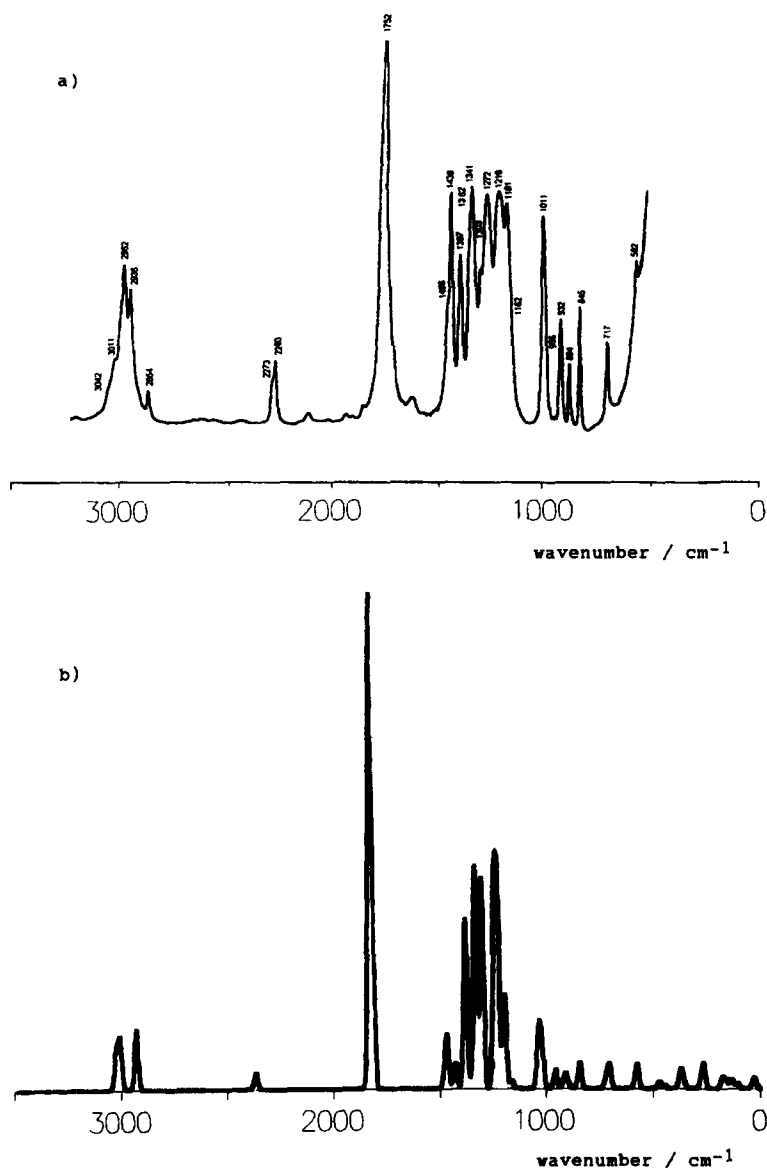
Fig. 3. (a) Experimental FT-IR spectrum of liquid MCA at room temperature. (b) 6-31G* predicted IR spectrum of MCA obtained by co-adding the calculated IR spectra for individual conformers (*syn/s-cis* and *skew/s-cis* forms; see Fig. 2). All gaussian functions used to simulate the bands are arbitrarily chosen to have a half band width equal to 30 cm⁻¹.

(that must be assigned to $\nu C \equiv N$ in the *syn* form) appears at 2259 cm⁻¹, being coincident with the lowest frequency band observed in the liquid phase.

In the case of the νC–H modes, the calculations predict that: (i) with the single exception of νCH_2 *as.*, that should appear at a slightly higher frequency in the *skew* form, all modes have similar frequencies in the two conformers; (ii) all vibrations should be considerably intense in Raman, while the two νCH_2 modes (in particular νCH_2 *as.*) should have low IR intensities. In consonance with the theoretical predictions, five Raman bands could be observed in this spectral region and assigned to the different νC–H modes, also taking into consideration the fact that
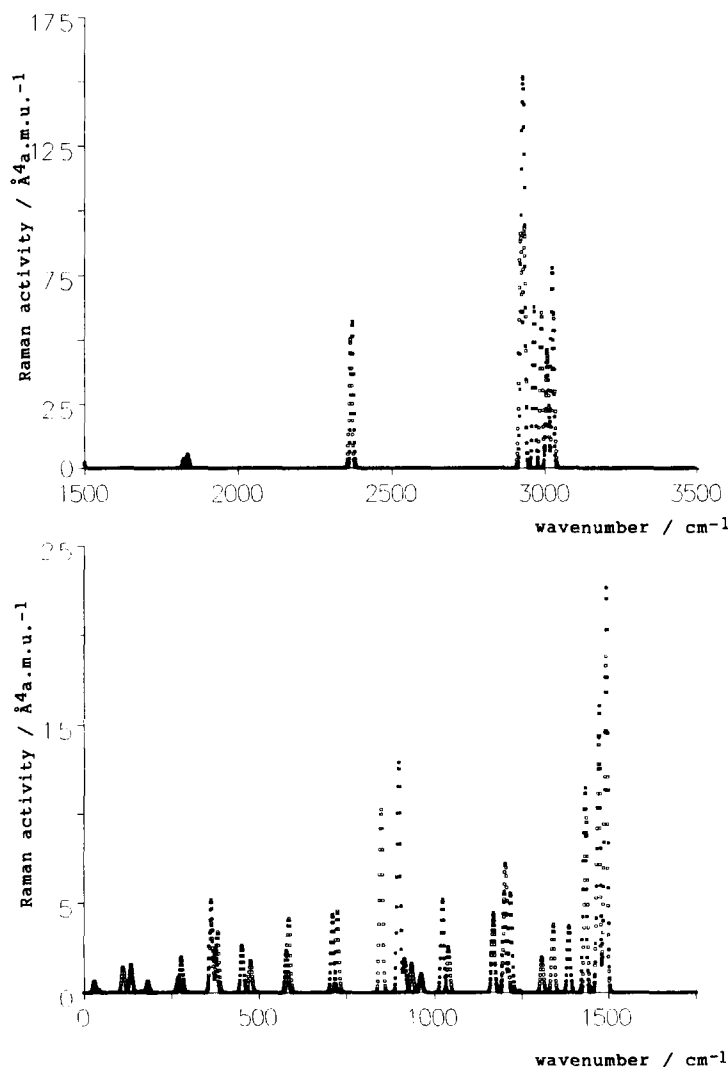
Fig. 4. 6-31G* calculated Raman spectra of the two spectroscopically observed conformers of MCA: ■ *syn/scis*; □ *skew/s-cis*. The calculated intensities of the bands due to the *syn/s-cis* conformer are multiplied by the factor 1.12 to account for the relative population of the two conformers at room temperature (see text). All gaussian functions used to simulate the bands are arbitrarily chosen to have a half band width equal to 10 cm⁻¹.

νCH$_2$ *as.* in the *skew* conformer must appear at a considerably higher frequency than in the *syn* form (Table 4). In turn, the IR spectrum shows only four bands in this spectral region that can be assigned to fundamental vibrations (the 2854 cm⁻¹ band, previously wrongly ascribed to νCH$_2$ *s.* [2], was here assigned to the first overtone of the δCH$_3$ *s.* bending vibration intensified by Fermi interaction with the

νCH$_3$ *s.* stretching mode, on the basis of the conclusions of previous systematic studies of this effect in methyl esters [21]).

3.5. 1700–1000 cm⁻¹ region

In this spectral region, the CH$_3$ bending and rocking modes, methylene scissoring, wagging and
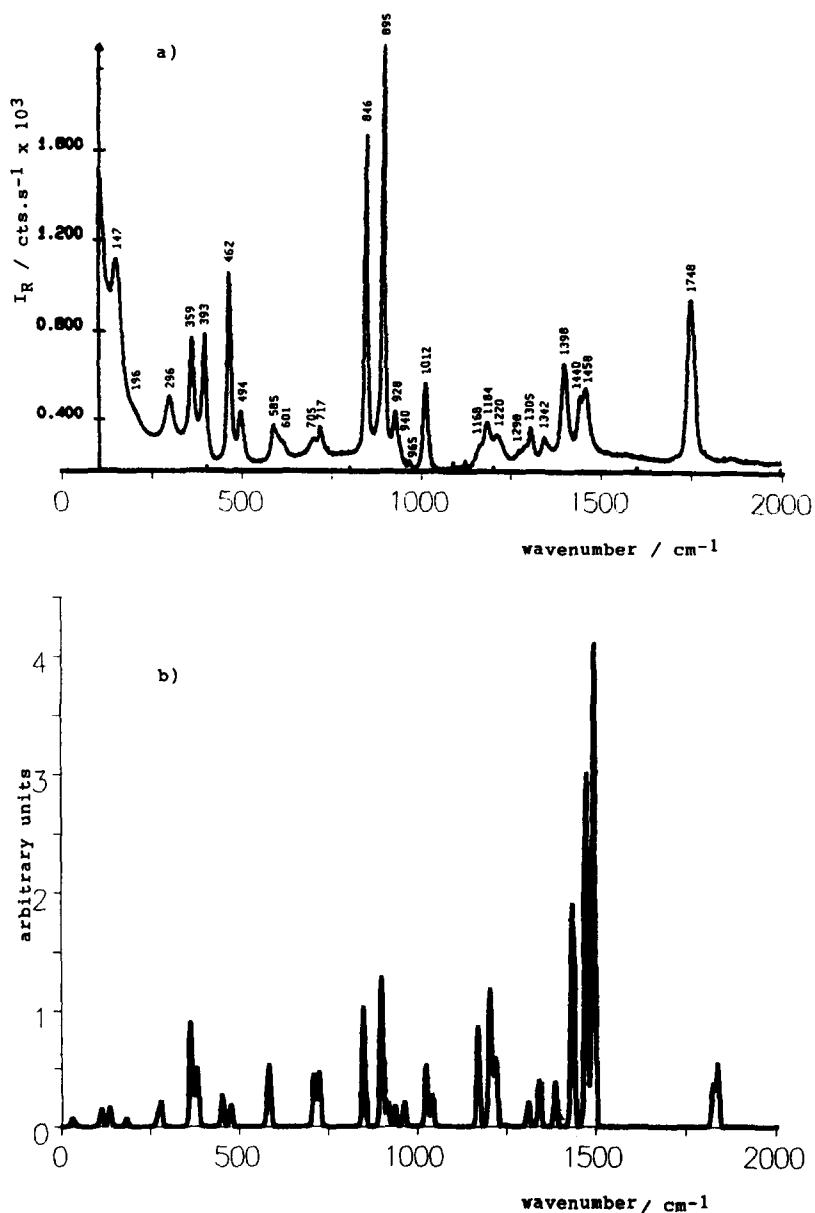
Fig. 5. (a) Experimental Raman spectrum of liquid MCA (~100–2000 cm⁻¹ region) at room temperature. (b) 6-31G* predicted IR spectrum of MCA (some region) obtained by co-adding the calculated Raman spectra for individual conformers (*syn/s-cis* and *skew/s-cis* forms) shown in Fig. 4.

twisting vibrations and the two carbon–oxygen single bonds' stretching modes (νC1–O and νO–C5) appear.

When compared with the previously proposed assignments [2], the assignments now made for the bands occurring in this spectral region agree in with concern to the δCH₃ bending modes, νC1–O and νO–C5, though in the case of the two νC–O vibrations the precise characterisation of the modes was not given in the previous study (instead, a general designation "skeletal stretching" was used [2]). On the other
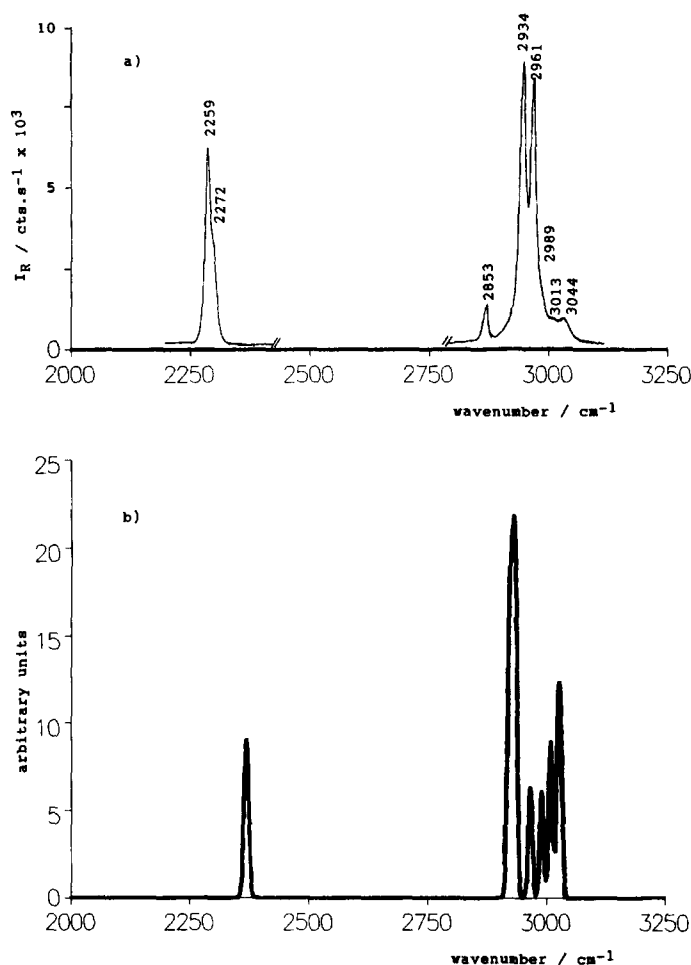
Fig. 6. (a) Experimental Raman spectrum of liquid MCA (2000–3250 cm^{-1} region) at room temperature. (b) 6-31G* predicted IR spectrum of MCA (some region) obtained by co-adding the calculated Raman spectra for individual conformers (*syn/s-cis* and *skew/s-cis* forms) shown in Fig. 4.

hand, the remaining modes are now reassigned taking into consideration the results of the theoretical predictions (Table 4). The following points deserve further comment:

1. Both in the IR and Raman spectra of the liquid MCA, two bands appear in this spectral region that originate in the *skew* conformer, thus increasing their relative intensities upon raising the temperature and being absent in the spectra of the crystal. These bands correspond to the ωCH_2 (IR, 1341 cm^{-1}; Raman, 1342 cm^{-1}) and νCl–O (IR, 1272 cm^{-1}; Raman, 1298 cm^{-1})modes;

2. All the other bands appearing in this spectral region have similar contributions from both conformers, except the relatively broad IR band at 1216 cm^{-1} (that has its Raman counterpart appearing at 1220 cm^{-1}), which is essentially due to the twCH_2 mode of the *syn* conformer. This later band is predicted by the calculations to be considerably more intense in IR than observed (Table 4) and it appears as a doublet of bands at 1218 and 1203 cm^{-1} in the IR spectrum of the crystalline sample. Thus, it seems that the broad band of the liquid phase IR spectrum due to the twCH_2 fundamental of the *syn* conformer corresponds in

Table 4
Experimental and calculated vibrational wavenumbers, intensities and potential energy distribution (PED) for methyl cyanoacetate (forms syn/s-cis and skew/s-cis)[a]

Approximate description	syn/s-cis						skew/s-cis					
	ν^{calc}	I_{ir}^{calc}	I_R^{calc}	ν_{ir}^{obs}	ν_R^{obs}	PED[b]	ν^{calc}	I_{ir}^{calc}	I_R^{calc}	ν_{ir}^{obs}	ν_R^{obs}	PED[b]
νCH3 as a'	3025	22.0	73.8	3042	3044	νCH3 as a' (99)	3029	19.0	63.6	3042	3044	νCH3 as a' (99)
νCH3 as a''	3008	24.8	43.8	3011	3013	νCH3 as a'' (100)	3009	25.0	46.8	3011	3013	νCH3 as a'' (100)
νCH2 as	2965	< 0.1	59.6	2962	2961	νCH2 as (101)	2989	0.1	64.3	2962	2989	νCH3 as (83) + νCH2 s (16)
νCH3 s	2932	29.8	86.4	2962	2961	νCH3 s (99)	2933	30.0	97.6	2962	2961	νCH3 s (99)
νCH2 s	2925	2.8	112.5	2936	2934	νCH2 s (100)	2920	0.9	95.7	2936	2934	νCH2 s (84) + νCH2 as (18)
νC≡N	2371	8.0	54.3	2260	2259	νC≡N (91)	2366	10.0	53.2	2273	2272	νC≡N (92)
νC=O	1836	305.0	5.0	1752	1748	νC=O (97)	1824	385.0	3.7	1752	1748	νC=O (96)
δCH3 as a'	1482	7.5	11.5	1456	1458	δCH3 as a' (79) + δCH3 s (11) + γCH3 a' (10)	1481	6.6	12.0	1456	1458	δCH3 as a' (79) + γCH3 s (11) + γCH3 a' (10)
δCH3 as a''	1477	5.4	17.9	1456	1458	δCH3 as a'' (95)	1477	5.7	16.7	1456	1458	δCH3 as a'' (95)
δCH3 s	1471	20.9	7.4	1438	1440	δCH3 s (80)	1470	18.0	6.5	1438	1440	δCH3 s (81)
δCH2	1431	17.5	10.9	1397	1398	δCH2 (112)	1435	8.8	10.4	1397	1398	δCH2 (113)
ωCH2	1385	171.0	3.5	1363	1364	ωCH2 (57) + νC3-C9 (20) + νC1-O (15) + δCH3 s (10)	1340	253.0	4.0	1341	1342	ωCH2 (46) + νC3-C9 (25) + νC1-O (25)
νC1-O	1242	431.0	0.1	1216	1220	νC1-O(50) + ωCH2(25) + γCH3 a'(13) + νO-C5(13)	1308	239.0	2.1	1272	1298	νC1-O (33) + ωCH2 (44)
tw CH2	1218	0.8	5.3	1216	1220	tw CH2 (92)	1209	28.0	2.1	1216	1220	tw CH2 (63) + γCH2 a' (23)
γCH3 a'	1200	57.6	5.4	1181	1184	γCH3 a' (66)	1203	22.0	6.8	1181	1184	γCH3 a' (53) + tw CH2 (21)
γCH3 a''	1168	3.9	4.2	1162	1168	δCH3 a'' (91)	1168	3.9	4.4	1162	1168	γCH3 a'' (91)
νO-C5	1023	36.8	4.9	1011	1012	νO-C5 (64) + νC3-C9 (12)	1040	68.0	2.7	1011	1012	νO-C5 (76) + νC3-C9 (13)
γCH2	961	10.4	0.9	966	965	γCH2(58) + νC=O (28)	962	9.4	1.1	966	965	γCH2 (51) + γC=O (15)
νC1-C3	915	14.6	1.8	932	928	νC1-C3 (59) + νO-C5 (22)	935	1.6	1.7	932	940	νC1-C3 (54) + γC=O (10)
νC3-C9	898	2.9	12.2	894	895	νC3-C9 (32) + νC1-O (15) + δCCC (11)	848	29.0	10.9	845	846	νC3-C9 (11) + νC1-O (30) + δO=C-O (14) + νO-C5 (13)
δO=C-O	709	20.6	4.1	717	705	δO=C-O (35) + δC-O-C (12) + δCCC (15)	723	14.0	4.8	717	717	δO=C-O(21) + νC1-O(22) + δCCC(13)
δC=O	578	11.6	2.2	582	585	γC=O (60) + τC1-O (17) + γCH2 (17)	584	16.0	4.4	(590)	601	γC=O (48) + τC1-O (16) + νC3-C9 (16)
δCC≡N	451	3.0	2.5	462	n.o.	δCC≡N (33) + νC3-C9 (21)	475	7.0	1.9	(492)	494	δCC≡N (29) + νC3-C9 (16) + γC=O (10) + δCC=O (10)
δCC=O	376	16.2	2.3	(391)	393	δCC=O (48) + δC-O-C (20) + δCC≡N (17)	381	2.6	3.6	(391)	393	δCC=O (37) + γCC≡N (40) + δCC≡N (22) + δC-O-C (13)
γCC≡N	362	2.6	4.9	(359)	359	γCC≡N (91) + γCH2 (20)	363	3.7	4.1	(359)	359	γCC≡N (62) + γCH2 (18) + δCC=O (12)
δC-O-C	278	11.8	1.9	(300)	296	δC-O-C (48) + δO-C-O (19) + δCC≡N (16) + δCC=O (11)	269	19.0	0.9	(300)	296	δC-O-C (54) + δCC≡N (17) + δO=C-O (15) + δCC≡N (14)
rO-CH3	163	7.6	< 0.1	n.o.	n.o.	rO-CH3 (62) + τC1-O(42) + γC=O(11)	145	1.3	0.1	(153)	147	rO-CH3 (81)
τC1-O	137	5.3	0.1	(153)	(153)	τC1-O (41) + rO-CH3 (39)	182	12.0	0.7	(~200)	196	τC1-O (53) + rO-CH3 (21) + δCCC (12) + δCC≡N (10)
δCCC	134	2.3	1.4	(153)	147	δCCC (54) + δCC≡N (25) + δCC=O (24)	111	5.3	1.5	(90)	n.o.	δCCC (38) + τC1-O (26) + δCC≡N (18) + δCC=O (10)
τC1-C3	39	3.0	0.2	n.o.	n.o.	τC1-C3 (90) + γC=O (10)	29	9.8	0.7	n.o.	n.o.	τC1-C3 (92)

[a] Wavenumbers in cm^{-1}; Infrared (ir) intensities in km mol^{-1}; Raman (R) scattering activities in Å^4 a.m.u.$^{-1}$; see Fig. 1 for atom numbering; ν, stretching; δ, bending; ω, wagging; tw, twisting; γ, rocking; τ, torsion; as., asymmetric; s., symmetric; n.o., not observed; calculated wavenumbers have been scaled down by multiplying the ab initio value by 0.9 (see text). IR wavenumbers shown in parenthesis were taken from ref. [2].

[b] PED values lower than 10% are not shown.

Table 5
Calculated wavenumbers, intensities and potential energy distribution (PED) for methyl cyanoacetate (forms *syn/s-trans* and *skew/s-trans*)[a]

Approximate description	*syn/s-trans* ν	I_{ir}	I_R	PED[b]	*skew/s-trans* ν	I_{ir}	I_R	PED[b]
νCH₃ as a'	3017	21.9	96.4	νCH₃ as a' (92)	3023	18.5	77.2	νCH₃ as a' (90)
νCH₃ as a"	2973	39.1	65.2	νCH₃ as a" (90) + νCH₂ as (11)	2997	3.2	70.0	νCH₂ s (82) + νCH₂ s (11)
νCH₂ as	2958	2.5	21.7	νCH₂ as (90) + νCH₃ as a" (11)	2992	24.5	33.2	νCH₃ as a" (83)
νCH₂ s	2921	9.0	130.3	νCH₂ s (92)	2933	4.2	111.4	νCH₂ s (84) + νCH₂ as (13)
νCH₃ s	2906	27.5	48.9	νCH₃ s (85)	2916	28.0	58.7	νCH₃ s (87)
νC≡N	2375	7.4	55.4	νC≡N (91)	2360	9.2	49.9	νC≡N (92)
νC=O	1854	419.0	12.3	νC=O (98)	1844	499.0	12.6	νC=O (97)
δCH₃ as a"	1494	9.3	18.9	δCH₃ as a' (101)	1495	14.2	14.7	δCH₃ as a" (92)
δCH₃ as a'	1485	17.4	14.4	δCH₃ as a' (85) + γCH₃ a' (10)	1486	20.3	13.0	δCH₃ as a' (75)
δCH₃ s	1481	5.7	5.1	δCH₃ s (100)	1481	4.6	4.0	δCH₃ s (94)
δCH₂	1435	16.4	8.0	δCH₂ (103)	1447	19.4	12.4	δCH₂ (106)
ωCH₂	1384	128.0	6.8	ωCH₂ (62) + νC3–C9 (18) + νC1–O (15)	1332	186.0	3.3	ωCH₂ (57) + νC1–O (22) + νC3–C9 (20)
νC1–O	1248	333.0	0.8	νC1–O (40) + γCH₃ a' (31) + ωCH₂ (19) + νO–C5 (11)	1297	171.0	3.1	νC1–O (33) + ωCH₂ (35) + tw CH₂ (12)
tw CH₂	1234	0.1	5.1	tw CH₂ (91)	1206	22.5	2.2	tw CH₂ (47) + γCH₃ a' (41)
γCH₃ a'	1165	114.0	4.4	γCH₃ a' (51) + νO–C5 (25) + νC1–O (17)	1164	75.6	5.3	γCH₃ a' (33) + tw CH₂ (25) + νO–C5 (15) + νC1–O (12)
νCH₃ a"	1160	3.1	4.2	γCH₃ a" (91)	1160	9.5	3.5	γCH₃ a" (83)
νO–C5	1082	83.2	3.1	νO–C5 (44) + δO=C–O (31) + νC3–C9 (16)	1089	80.2	2.6	νO–C5 (55) + δO=C–O (25) + νC3–C9 (16)
γCH₂	957	11.9	1.1	γCH₂ (58) + γC=O (26)	955	6.8	2.4	γCH₂ (67)
νC1–C3	944	28.7	1.2	νC1–C3 (68)	923	3.7	2.5	νC1–C3 (64) + γC=O (10)
νC3–C9	834	6.7	10.0	νC3–C9 (45) + δCCC (17) + νO–C5 (11)	820	26.5	6.8	νC3–C9 (20) + νC1–O (20) + γC=O (15) + δCCC (13)
δO=C–O	599	12.6	6.3	δO=C–O (39) + νO–C5 + νC1–O(13)	683	20.3	6.2	γC=O(27) + νC3–C9(15) + νC1–C3(15) + δO=C–O(13) + νO–C5(13)
γC=O	545	11.5	1.9	γC=O (86) + γCH₂ (25) + tw CH₂ (14)	558	25.3	2.7	δO=C–O (34) + γC=O (28)
δCC=O	494	9.3	0.8	δCC=O (13) + δC–O–C (41) + νC3–C9 (20) + δO=C–O (12)	460	5.9	0.9	δCC≡O (51) + δCC≡N (16) + δC–O–C (11) + δO=C–O (11) + γCH₂ (10)
δCC≡N	411	7.6	2.6	δCC≡N (47) + δCC=O (45) + δC–O–C (22)	429	4.3	1.9	δCC≡N (47) + δC–O–C (36) + δCC=O (33) + δCC≡N (25)
γCC≡N	365	2.5	4.4	γCC≡N (85) + γCH₂ (23)	375	0.9	4.8	γCC≡N (74) + γCH₂ (10)
δC–O–C	265	0.6	1.2	δC–O–C (44) + δO=C–O (10)	286	0.8	0.7	δC–O–C (54) + δCC=O (15)
τO–CH₃	190	0.7	0.5	τO–CH₃ (116)	181	5.9	0.2	τO–CH₃ (92)
δCCC	146	4.4	1.7	δCCC (55) + δCC≡N (30) + δCC=O (20)	145	11.1	2.6	δCCC (50) + δCC≡N (31) + γCC≡N (11)
τC1–O	84	5.4	0.1	τC1–O (69) + τC1–C3 (37)	79	3.1	1.0	τC1–O (46) + τC1–C3 (54)
τC1–C3	39	7.3	0.5	τC1–C3 (48) + γC1–O (15) + τC1–O (13)	38	11.7	1.1	τC1–C3 (41) + τO–CH₃ (28) + τC1–O (10)

[a] Wavenumbers in cm⁻¹; Infrared (ir) intensities in km mol⁻¹; Raman (R) scattering activities in Å⁴ a.m.u.⁻¹; see Fig. 1 for atom numbering; ν, stretching; δ, bending; ω, wagging; tw, twisting; γ, rocking; τ, torsion; as., asymmetric; s., symmetric; wavenumbers have been scaled down by multiplying the ab initio value by 0.9 (see text).
[b] PED values lower than 10% are not shown.

fact to an unresolved Fermi doublet, most probably resulting from the interaction with the νO–C5 + δC–O–C combination mode. This interpretation was considered in the simulation of the IR predicted spectrum of MCA shown in Fig. 3, where an unresolved doublet of bands due to this interaction, each one with half of the total intensity calculated for the twCH$_2$ IR band, has been plotted instead of a single band. Indeed, such procedure enables us to attain a much better fit between the predicted and experimentally observed IR spectra;

3. The results of the normal coordinate analysis indicate that the ωCH$_2$ and νC1–O vibrations are considerably mixed, in particular in the case of the non-symmetric *skew* conformer. On the other hand, the νO–C5 stretching mode, and all the methyl bending and rocking modes have a clear prevalence of a single coordinate (this is particularly evident in the case of the *syn* form, Table 4);

4. The calculations predict νC1–O to occur at higher frequencies than observed ($\Delta\nu$C1–O$_{(cal-exp)}$ ~30 cm^{-1}). Indeed, the same trend can also be noticed for both νC≡N ($\Delta\nu$C≡N$_{(cal-exp)}$ ~100 cm^{-1}) and νC=O ($\Delta\nu$C=O$_{(cal-exp)}$ ~80 cm^{-1}). This is a direct consequence of the intermolecular interactions present in the condensed phases, that affect mainly the more polarised bonds (the theoretical data assumes the molecule isolated in the vacuum), and these results follow the trend previously reported for similar studies in other carboxylic compounds [1,13,15]. It must be stressed that these are in fact the three vibrational modes that have their frequencies most overestimated by calculations, and that, as a trend, this over-estimation is slightly larger for the more polar *syn* conformer (Table 4).

3.6. Region below 1000 cm^{-1}

In this spectral region the γCH$_2$ rocking mode, the two νC–C stretching vibrations, and all skeletal bending and torsional modes appear.

In the Raman spectrum of liquid MCA it was possible to observe in this spectral region five bands that are due to the *skew* conformer: the intense and well resolved band at 846 cm^{-1} (IR: 845 cm^{-1}),

assigned to νC3–C9, the bands at 717, 601 and 494 cm^{-1}, here assigned to δO=C–O, γC=O and δC–C≡N, respectively, and the shoulder at 196 cm^{-1}, tentatively assigned to the τC1–O torsional mode. The assignments now made for this spectral region, which are fully supported by the theoretical results, are considerably different and improve significantly the tentative assignments made in ref. [2].

Using the temperature dependence of the relative intensities of the pairs of bands at 894/845 cm^{-1} (IR) and 895/846 cm^{-1} and 462/494 cm^{-1} (Raman), over the temperature range 298–333K (above 333K the compound starts to decompose), an average value of 2.0 ± 0.2 kJ mol^{-1} for ΔH$_{(skew-syn)}$ was obtained for MCA in the liquid phase, corresponding to a relative *syn/skew* population ratio, at room temperature, equal to 1.12. The experimentally measured enthalpy difference between the two conformers (that lies in between the previously reported values: 4.06 kJ mol^{-1} [2]; 1.46 kJ mol^{-1} [3]), is higher than the conformer energy difference calculated for the isolated molecule situation ($\Delta E_{(skew-syn)} = 0.94$ kJ mol^{-1}), a result that is consistent with an additional stabilisation in the condensed phase of the more polar *syn* conformer.

Acknowledgements

References

[1] J.M.F. Neta, Estudo Estrutural e Espectroscópico de Compostos Carbonílicos α-ciano-substituídos, Departamento de Química, Universidade de Coimbra, Internal Report 1997 (and references therein).

[2] S.W. Charles, G.I.L. Jones, N.L. Owen, J. Chem. Soc. Faraday Trans II 69 (1973) 1454.

[3] C. Maury, J. Petrissans, J. Mol. Struct. 246 (1991) 267.

[4] R. Das, S. Chattopadhayay, G.S. Kastha, Indian J. Phys. 53B (1979) 297.

[5] W.J. Hehre, R. Ditchefield, J.A. Pople, J. Chem. Phys. 56 (1972) 2257.

[6] M.J. Frisch, G.W. Trucks, H.B. Schlegel, P.M.W. Gill, B.G. Johson, M.W. Wong, J.B. Foresman, M.A. Robb, M. Head-Gordon, E.S. Replogle, R. Gomperts, J.L. Andres,

K. Raghavachari, J.S. Binkley, C. Gonzalez, R.L. Martin, D.J. Fox, D.J. Defrees, J Baker, J.J.P. Stewart, J.A. Pople, GAUSSIAN 92/DFT (Revision G.2), Gaussian Inc., Pittsburgh PA, 1993.

[7] H.B. Schlegel, Ph.D. Thesis, Queen's University, Kingston, Ontario, Canada, 1975.

[8] R. Fausto, TRANSFORMER (version 2.0), Departamento de Química, Universidade de Coimbra, Portugal, 1997.

[9] M.D.G. Faria, R. Fausto, BUILD-G and VIBRAT, Departamento de Química, Universidade de Coimbra, Portugal, 1990 (These programs incorporate several routines from programs GMAT and FPERT, H. Fuher, V.B. Kartha, K.G. Kidd, P.J. Krueger, H.H. Mantsch, Natl. Res. Council Can. Bull. 15(1976) 1.

[10] J.J.C. Teixeira-Dias, R. Fausto, J. Mol. Struct. 144 (1986) 199.

[11] R. Fausto, J.J.C. Teixeira-Dias, J. Mol. Struct. (Theochem.) 150 (1987) 381.

[12] R. Fausto, J.J.C. Teixeira-Dias, J. Mol. Struct. 144 (1986) 215, 225, 241.

[13] A. Kulbida, R. Fausto, J. Chem. Soc. Faraday Trans. 89 (1993) 4257.

[14] R. Fausto, J. Mol. Struct. (Theochem.) 315 (1994) 123.

[15] R. Fausto, A. Kulbida, O. Schrems, J. Chem. Soc. Faraday Trans. 91 (1995) 3755.

[16] R. Fausto, F.P.S.C. Gil, J.J.C. Teixeira-Dias, J. Chem. Soc. Faraday Trans. 89 (1993) 3235.

[17] A. Kulbida, A. Nosov, J. Mol. Struct. 265 (1992) 17.

[18] P.J. Tonge, V.E. Andersson, R. Fausto, M. Kim, M. Pusztay-Carey, P.R. Carey, Biospectroscopy 1 (1995) 387.

[19] L.A.E. Batista de Carvalho, J.J.C. Teixeira-Dias, R. Fausto, J. Mol. Struct. (Theochem.) 208 (1990) 109.

[20] R. Fausto, Ph.D. Thesis, Departamento de Química, Universidade de Coimbra, Coimbra, Portugal, 1988.

[21] J.C. Lavalley, N. Sheppard, Spectrochim. Acta 28A (1972) 2091.